

Basic Analytical and Geometric Synthesis of Conic Convolute Helical Surfaces of Spatial Rack Drives. Software and Graphic Study

Emilia Abadjieva^{1,2}

Institute of Mechanics- Bulgarian Academy of Sciences, Acad. G. Bonchev Str, block 4, Sofia, Bulgaria¹

Center of Competence MIRACLe – Mechatronics Clean Technologies, Sofia, Bulgaria²

abadjieva@gmail.com

Abstract: This study treats a study oriented to the basic synthesis of the conic convolute helicoid. On the base of the elaborated mathematical model, the written equations show a theoretical possibility, depending on the basic geometrical characteristics of the designed conic convolute worm, to generate the active flanks of the helical teeth as parts of these conic convolute helicoids. Analytical dependences of the cross-section and the axial section of the conic convolute surfaces are obtained. These relations, as well as the performed studies of the graphic images of these sections, precede the process of constructing the algorithms for computer synthesis and design of these conic helical surfaces. The realized studies of the graphic images of these sections are the basis of the algorithms for computer synthesis and design of these conical helical surfaces. The appearance of singular points on these surfaces is examined, which is of particular importance for their technological synthesis. Based on the developed algorithm, a computer program for the synthesis and visualization of conic helical surfaces is realized and illustrated.

Keywords: SPATIAL RACK DRIVES, CONIC LINEAR HELICOIDS, GEOMETRIC CHARACTERISTICS

1. Introduction

In the group of gear mechanisms, a certain significance for the technique has spatial rack mechanisms, transforming motions of type ($R \leftrightarrow T$) [1]. The reason for this is that, as a mechanical system, this type of gear drives does not have an alternative for cases of motions' transformation with high power, as there are an alternative for small power and displacements, which are electrical drives with electronic control. Hydraulic transmissions represent a definite alternative, but high-tech and expensive servo systems are used to achieve high positioning accuracy.

The successful implementation of the spatial rack drives with new kinematic and strength characteristics into the techniques is retained by the insufficient studying of the general principles of this transformation, due to the lack of offered specific approaches to mathematical modeling, oriented to their synthesis.

The global structure of every mathematical model of the above-considered type is determined by [1-3]:

- The designation of the three-link mechanism under the preliminary defined law of motions transformation;
- the placement of the characteristic axes of the movable links and the nature of the conjugation of the elements of high kinematic joints (with a point or linear tangential contact);
- the technological devices, connected with the choice of the geometry of the generating (instrumental) surfaces and the chosen principle for generation by T. Olivier.

Further below, two ways of generation of the active tooth surfaces Σ_2 of the gear rack (link $i=2$) of the studied mechanism are marked [1 - 3]:

- Σ_2 is generated by enveloping in accordance with the second principle of T. Olivier; Σ_2 is cut with an instrument J , which generating (enveloping) surfaces Σ_j are geometrically identical with the tooth surfaces Σ_1 of the rotating link $i=1$, i.e. $\Sigma_j \equiv \Sigma_1$; the cutting instrument J occupies the same relative placement towards the blanks of the link $i=2$; the relative motion of the instrument J towards the blank of the link $i=2$ is the same as it is of Σ_1 towards Σ_2 when there are work mating. Hence, the generated surfaces Σ_2 have a line contact with Σ_1 .

- Σ_2 is a cylindrical surface, for which it is easy to determine the analytical type of its normal section, which is the normal profile of the tooth of the gear rack. When the orientation of the longitudinal line of the tooth and the geometry of its normal profile are known, then Σ_2 can be generated by copying. In this case also Σ_1 and Σ_2 contact in a line.

In the current study, the first approach to the synthesis of these motions' transformers is applied. This determines the importance of the written here theory, which is referred to the synthesis of the surfaces $\Sigma_j \equiv \Sigma_1$ of the conic linear helicoids.

To realize a complete study of the conic convolute helical surfaces are written analytical descriptions of their cross-sections and axial sections. Other important characteristics of the technological synthesis of the spatial rack drives are the conditions for the appearance of singular points on the conic linear helical surfaces. In the study, this topic is briefly explained.

2. Synthesis of Conic Linear Helical Surfaces

Generation of Conic Convolute Mechanisms. The helicoids and especially the linear helicoids are widely applied as active tooth surfaces of spatial transmissions with crossed axes, both in work meshing and instrumental meshing conditions. Such choice of the active tooth surfaces for these gears is determined by technological manufacturing, especially when their synthesis is realized under the second Oliver's principle [1, 4 - 7]. In many cases (like the manufacture of the cylindrical worm gear and Spiroid¹ and Helicon gear-set), these surfaces are the only alternative.

On Fig. 1 is illustrated the generation of right-handed conic convolute helicoids $\Sigma_1^{(j)}$ ($j=1, 2$) determined by different geometrical characteristics of the helical teeth (treads) of the particular gear mechanism [8 - 10]. The process of helical surfaces' generation is considered in a fixed coordinate system $S_p^{(j)}(O_p^{(j)}, x_p^{(j)}, y_p^{(j)}, z_p^{(j)})$ and it is as follows. The generatrix of $\Sigma_1^{(j)}$ doesn't cross the axis $O_p^{(j)}z_p^{(j)}$ which coincides with the geometric axis of the gear. $\Sigma_1^{(j)}$ and $O_p^{(j)}z_p^{(j)}$ conclude an angle $0,5\pi < \xi^{(j)} < \pi$. The line $L^{(j)}$ belongs to a plane $T^{(j)}$, which

¹ Spiroid and Helicon are trademarks registered by the Illinois Tool Works, Chicago, Ill.

is tangential to the directed circle cylinder $C^{(j)}$. The generation of the conic convolute helicoid $\Sigma_1^{(j)}$ by the line $L^{(j)}$ is realized by two generatrix motions [2, 8, 11]: axial helical motion along the longitudinal axis $O_p^{(j)}z_p^{(j)}$ with parameter $p_s^{(j)} = const.$;

crossed helical motion in the plane $\Sigma^{(j)}$, perpendicular to the axis $O_p^{(j)}z_p^{(j)}$ with parameter $p_t^{(j)} = const.$ Here, it will be noted that $\Sigma_1^{(1)}$ is conic convolute helicoid surface, which is oriented to the positive direction of the axis $O_p^{(1)}z_p^{(1)}$, and $\Sigma_1^{(2)}$ is the helicoid, turned along the negative direction of the $O_p^{(2)}z_p^{(2)}$.

The vector equation of the conic convolute helicoid surface $\Sigma_1^{(j)}$, in accordance with Fig. 1, has the form [1, 2, 11]:

$$\bar{\rho}_1^{-(j)} = r_0^{-(j)} + s^{-(j)} + t^{-(j)} + u^{-(j)}, \quad (1)$$

where $\bar{\rho}_1^{-(j)}$ is a radius-vector of a point $N^{(j)}$ that belongs to the conic convolute helicoid $\Sigma_1^{(j)}$; $r_0^{-(j)}$ - radius-vector of the directed cylinder $C^{(j)}$; $\mathcal{G}^{(j)}$, $u^{(j)}$ - coordinates of the helical surface $\Sigma_1^{(j)}$; $s^{(j)} = p_s^{(j)}\mathcal{G}^{(j)}$ - axial motion of the generatrix $L^{(j)}$; $t^{(j)} = p_t^{(j)}\mathcal{G}^{(j)}$ - crossed displacement (tangential to the directed cylinder $C^{(j)}$) of the generatrix line $L^{(j)}$.

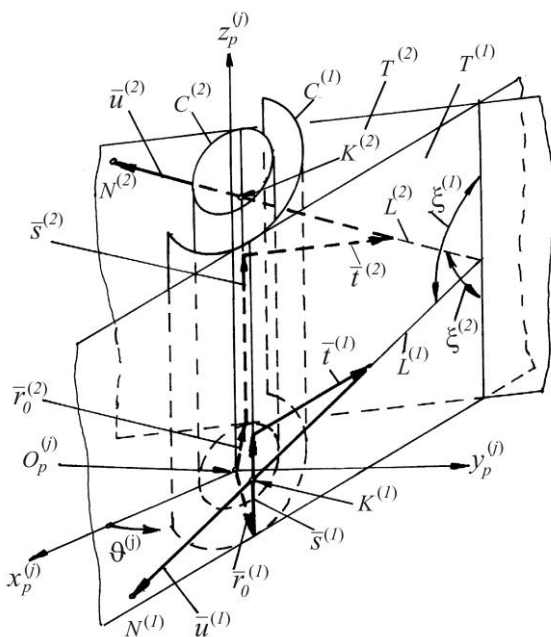


Fig. 1 Conic convolute helicoids generation

When (1) is written in a coordinate system $S_p^{(j)}$ it is obtained:

$$\begin{aligned} x_p^{(j)} &= r_0^{(j)} \cos \mathcal{G}^{(j)} \pm A \sin \mathcal{G}^{(j)}, \\ y_p^{(j)} &= r_0^{(j)} \sin \mathcal{G}^{(j)} \mp A \cos \mathcal{G}^{(j)}, \\ z_p^{(j)} &= p_s^{(j)} \mathcal{G}^{(j)} \pm u^{(j)} \cos \xi^{(j)}, \\ A &= (u^{(j)} \sin \xi^{(j)} - p_t^{(j)} \mathcal{G}^{(j)}), \end{aligned} \quad (2)$$

For equation systems (2) the upper signs and $j = 1$ refer to the $\Sigma_1^{(1)}$, and the lower and $j = 2$ refer to the $\Sigma_1^{(2)}$.

Substituting in (2)

$$R_0^{(j)} = u^{(j)} - \frac{p_t^{(j)} \mathcal{G}^{(j)}}{\sin \xi^{(j)}} \quad (3)$$

and

$$p^{(j)} = p_s^{(j)} \pm p_t^{(j)} \cot \xi^{(j)}$$

it is obtained

$$\begin{aligned} x_p^{(j)} &= r_0^{(j)} \cos \mathcal{G}^{(j)} \pm R_0^{(j)} \sin \xi^{(j)} \sin \mathcal{G}^{(j)}, \\ y_p^{(j)} &= r_0^{(j)} \sin \mathcal{G}^{(j)} \mp R_0^{(j)} \sin \xi^{(j)} \cos \mathcal{G}^{(j)}, \\ z_p^{(j)} &= p^{(j)} \mathcal{G}^{(j)} \pm R_0^{(j)} \cos \xi^{(j)}; \end{aligned} \quad (4)$$

Equation (4) represents the conic convolute helicoid surface $\Sigma_1^{(j)}$ as a cylindrical one with helical parameter $p^{(j)} = const.$ and coordinates $\mathcal{G}^{(j)}$ and $R_0^{(j)}$. (The point $K^{(j)}$ is the accounting origin of coordinate $R_0^{(j)}$. $C^{(j)}$ and plane $T^{(j)}$ are contacting in this generatrix $L^{(j)}$). The point $K^{(j)}$ is considered as a point from the directed helical line $\bar{\rho}_0^{(j)} = \bar{\rho}_0^{(j)}(\mathcal{G}^{(j)})$ on the $C^{(j)}$.

For the synthesis of the conic linear helicoids (conic convolute, conic involute, and conic Archimedean) are written three computer programs [1] with analogical (typified) structure and organization of the calculated process. Here and further, it is illustrated the application of these programs, when is realized computer synthesis and visualization of the three types of conic linear helicoids (see Fig. 2, Fig. 3, Fig. 4).

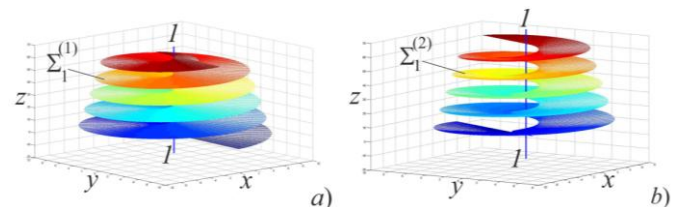


Fig. 2 Spatial conic convolute gear: a) conic convolute right-handed worm $\Sigma_1^{(1)} \Rightarrow \xi^{(1)} = 95^\circ$, $r_0^{(1)} = 0,90 \text{ mm}$; $u^{(1)} \in [0,10]$, $\mathcal{G}^{(1)} \in [0,5\pi]$; b) $\Sigma_1^{(2)} \Rightarrow \xi^{(2)} = 125^\circ$, $r_0^{(2)} = 1,19 \text{ mm}$; $u^{(2)} \in [0,10]$, $\mathcal{G}^{(2)} \in [0,5\pi]$

Conic involute helical surfaces generation. It is known [1, 2, 11] that each developable surface is a cylindrical one, conic one, or a locus of the tangent lines to an arbitrary curve and vice versa - each cylindrical, conic or a surface representing the locus of tangent lines to a curve is a developable surface.

The specific for each developable surface is, that the parameter of distribution is equal to zero, i.e.

$$\begin{aligned} h^{(j)} &= p^{(j)} + r_0^{(j)} \cot \xi^{(j)} = 0, \\ \text{or} \\ \cot \xi^{(j)} &= -\frac{p^{(j)}}{r_0^{(j)}} \end{aligned} \quad (5)$$

After observing condition (5), equation (4) describes the conic involute helicoid (Fig. 3), which is given in the form:

$$\begin{aligned} x_p^{(j)} &= r_0^{(j)} \cos \mathcal{G}^{(j)} \pm R_0^{(j)} \cos \lambda_0^{(j)} \sin \mathcal{G}^{(j)}, \\ y_p^{(j)} &= r_0^{(j)} \sin \mathcal{G}^{(j)} \mp R_0^{(j)} \cos \lambda_0^{(j)} \cos \mathcal{G}^{(j)}, \\ z_p^{(j)} &= p^{(j)} \mathcal{G}^{(j)} \mp R_0^{(j)} \sin \lambda_0^{(j)}, \end{aligned} \quad (6)$$

where $R_0^{(j)} = u^{(j)} - \frac{p_t^{(j)} \mathcal{G}^{(j)}}{\cos \lambda_0^{(j)}}$, $p^{(j)} = p_s^{(j)} \mp p_t^{(j)} \tan \lambda_0^{(j)}$

and $\lambda_0^{(j)} = \xi^{(j)} - \pi/2$ is a spiral angle [1, 11] for the directed helical line on the cylinder $C^{(j)}$. In this case, the cylinder $C^{(j)}$ is called a basic cylinder.

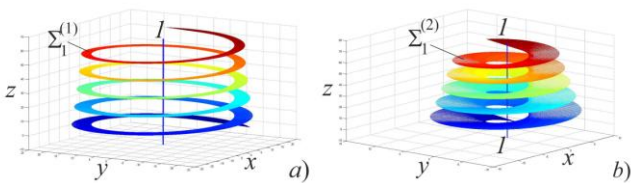


Fig. 3 Spatial conic involute mechanism: a) conic involute right-handed worm $\Sigma_1^{(1)} \Rightarrow \xi^{(1)} = 95^\circ$, $r_0^{(2)} = 18,40$ mm; $u^{(1)} \in [-5, 15]$, $\mathcal{G}^{(1)} \in [0, 5\pi]$; b) $\Sigma_1^{(2)} \Rightarrow \xi^{(2)} = 125^\circ$, $r_0^{(2)} = 2,84$ mm; $u^{(2)} \in [-5, 15]$, $\mathcal{G}^{(2)} \in [0, 5\pi]$

Conic Archimedean helical surfaces generation. The conic Archimedean helicoid is obtained when the generatrix $L^{(j)}$ (see Fig. 4) crosses the axis $O_p^{(j)} z_p^{(j)}$, i.e. when $r_0^{(j)} = 0$.

Then from (2), it is obtained:

$$\begin{aligned} x_p^{(j)} &= \pm(u^{(j)} \sin \xi^{(j)} - p_t^{(j)} \mathcal{G}^{(j)}) \sin \mathcal{G}^{(j)}, \\ y_p^{(j)} &= \mp(u^{(j)} \sin \xi^{(j)} - p_t^{(j)} \mathcal{G}^{(j)}) \cos \mathcal{G}^{(j)}, \\ z_p^{(j)} &= p_s^{(j)} \mathcal{G}^{(j)} \pm u^{(j)} \cos \xi^{(j)}. \end{aligned} \quad (7)$$

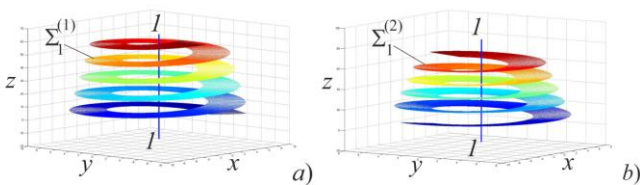


Fig. 4 Spatial conic Archimedean mechanism: a) conic Archimedean right-handed worm $\Sigma_1^{(1)} \Rightarrow \xi^{(1)} = 95^\circ$, $u^{(1)} \in [6, 10]$, $\mathcal{G}^{(1)} \in [0, 5\pi]$; b) $\Sigma_1^{(2)} \Rightarrow \xi^{(2)} = 125^\circ$, $u^{(2)} \in [6, 10]$, $\mathcal{G}^{(2)} \in [0, 5\pi]$

The curvilinear coordinate $\mathcal{G}^{(j)}$ in (7) represents the angle on which rotates the normal vector $\bar{r}_0^{(j)}$ to the axial plane (determined by the $L^{(j)}$ and $O_p^{(j)} z_p^{(j)}$). If it is noted with $\mathcal{G}_a^{(j)} = \mathcal{G}^{(j)} + \pi/2$, the angle, that the plane $(L^{(j)}, O_p^{(j)} z_p^{(j)})$ concludes with the plane $(O_p^{(j)} x_p^{(j)} z_p^{(j)})$, then the equation systems (7) turn into:

$$\begin{aligned} x_p^{(j)} &= \mp[B] \cos \mathcal{G}_a^{(j)}, \\ y_p^{(j)} &= \mp[B] \sin \mathcal{G}_a^{(j)}, \\ z_p^{(j)} &= p_s^{(j)} (\mathcal{G}_a^{(j)} - \pi/2) \pm u^{(j)} \cos \xi^{(j)}, \\ B &= u^{(j)} \sin \xi^{(j)} - p_t^{(j)} (\mathcal{G}_a^{(j)} - \pi/2). \end{aligned} \quad (8)$$

3. Basic Geometric Characteristics of the Conic Convolute Surface

Parameter of Distribution. It is known [6, 11, 12] that the main characteristic of surfaces with rectilinear generatrices is their parameter of the distribution. When surfaces of such type are generated, the rectilinear generatrix passes from its initial position to an infinitely closed vicinal position, rotating at an angle and displacing at some distance. These two quantities are infinitely small, but their ratio has its limits, which is titled a *parameter of the distribution*.

Following Fig. 5 the transition of the rectilinear generatrix $L^{(j)}$, (which is characterized by the parameter \mathcal{G}), in a position L' , characterized by infinitely close value $\mathcal{G} + \Delta\mathcal{G}$, then it rotates to an angle $\Delta\varphi$ and deviates from its initial position to a distance $\Delta\lambda = MM'$. As has been already mentioned, these values are infinitely small, and their ratio tends to a certain limit, which is called a parameter of distribution [12]:

$$h = \lim_{\Delta\mathcal{G} \rightarrow 0} \frac{\Delta\lambda}{\Delta\varphi} \quad (9)$$

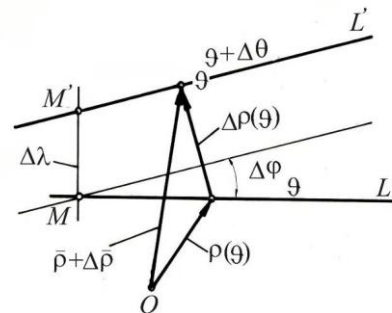


Fig. 5 Transition of the generatrix L into an infinitely close position L'

To determine the distribution parameter $\Sigma^{(j)}$ of the conic convolute helical surface $\Sigma_1^{(j)}$, the vector equation (1) is presented of the type [2]:

$$\bar{\rho}_1^{(j)} = \bar{\rho}_0^{(j)} (\mathcal{G}^{(j)}) + R_0^{(j)} \bar{l}^{(j)}, \quad (10)$$

where $\bar{\rho}_0^{(j)} = \bar{\rho}_0^{(j)} (\mathcal{G}^{(j)}) \{ \chi_1^{(j)}, \chi_2^{(j)}, \chi_3^{(j)} \}$ is an equation of a directed helical line on the directed cylinder $C^{(j)}$; $\chi_1^{(j)}, \chi_2^{(j)}, \chi_3^{(j)}$ - projection of the vector $\bar{\rho}_0^{(j)}$ in the coordinate system $S_p^{(j)}$; $\bar{l}^{(j)} \{ l_1^{(j)}, l_2^{(j)}, l_3^{(j)} \}$ - directed unit vector of the generatrix line $\Sigma^{(j)}$; $l_1^{(j)}, l_2^{(j)}, l_3^{(j)}$ - projections of $\bar{l}^{(j)}$ in the coordinate system $S_p^{(j)}$.

For the case illustrated in Fig. 1, it is written:

$$\begin{aligned} \chi_1^{(j)} &= r_0^{(j)} \cos \vartheta^{(j)}, \quad \chi_2^{(j)} = r_0^{(j)} \sin \vartheta^{(j)}, \\ \chi_3^{(j)} &= p^{(j)} \cdot \vartheta^{(j)}, \\ l_1^{(j)} &= \pm \sin \xi^{(j)} \sin \vartheta^{(j)}, \quad l_2^{(j)} = \mp \sin \xi^{(j)} \cos \vartheta^{(j)}, \\ l_3^{(j)} &= \pm \cos \xi^{(j)}, \end{aligned} \quad (11)$$

Then, applying (9), as it is shown in [6, 12], for the studied conic convolute helical surface it can be written:

$$h^{(j)} = \frac{\begin{vmatrix} d\chi_1^{(j)} & l_1^{(j)} & dl_1^{(j)} \\ d\chi_2^{(j)} & l_2^{(j)} & dl_2^{(j)} \\ d\chi_3^{(j)} & l_3^{(j)} & dl_3^{(j)} \end{vmatrix}}{(dl_1^{(j)})^2 + (dl_2^{(j)})^2 + (dl_3^{(j)})^2}. \quad (12)$$

For $\Sigma^{(j)}$ from (12) it is obtained the following:

$$h^{(j)} = p^{(j)} + r_0^{(j)} \cot \xi^{(j)}. \quad (13)$$

Cross section of the conic convolute helicoid

The equation of the illustrated in Fig. 1 conic convolute helical surfaces with the plane $O_p^{(j)} x_p^{(j)} y_p^{(j)}$, i.e. when $z_p^{(j)} = 0$, has the following parametric form:

$$\rho_p^{(j)} = \sqrt{(r_0^{(j)})^2 + \left(\frac{p^{(j)} \vartheta^{(j)}}{\cot \xi^{(j)}}\right)^2}. \quad (14)$$

In Cartesian coordinates, the cross-section of the convolute helicoids $\Sigma_I^{(j)}$, when $z_p^{(j)} = C_{z_p}^{(j)} = const.$, is described with the following system of equations:

$$\begin{aligned} x_p^{(j)} &= r_0^{(j)} \cos \vartheta^{(j)} + C \vartheta^{(j)} \sin \vartheta^{(j)}, \\ y_p^{(j)} &= r_0^{(j)} \sin \vartheta^{(j)} - C \vartheta^{(j)} \cos \vartheta^{(j)}, \end{aligned} \quad (15)$$

$$C = [\tan \xi^{(j)} \left(\frac{C_{z_p}^{(j)}}{\vartheta^{(j)}} - p_s^{(j)} \right) \mp p_t^{(j)}].$$

Equations (15) are written in the form:

$$\begin{aligned} x_p^{(j)} &= r_0^{(j)} \cos \vartheta^{(j)} + b^{(j)} \vartheta^{(j)} \sin \vartheta^{(j)}, \\ y_p^{(j)} &= r_0^{(j)} \sin \vartheta^{(j)} - b^{(j)} \vartheta^{(j)} \cos \vartheta^{(j)}, \end{aligned} \quad (16)$$

where $b^{(j)} = \tan \xi^{(j)} \left(\frac{C_{z_p}^{(j)}}{\vartheta^{(j)}} - p_s^{(j)} \right) \mp p_t^{(j)}$.

The essence of the cross-section of the conic convolute helicoid can be clarified by introducing circular vector functions [4, 6] $\bar{l}^{(j)} = \bar{l}^{(j)}(\vartheta^{(j)})$ and $\bar{g}^{(j)} = \bar{g}^{(j)}(\vartheta^{(j)})$, for which the condition is fulfilled:

$$\begin{aligned} \bar{l}^{(j)} &= \bar{i}_p^{(j)} \cos \vartheta^{(j)} + \bar{j}_p^{(j)} \sin \vartheta^{(j)}, \\ \bar{g}^{(j)} &= -\bar{i}_p^{(j)} \sin \vartheta^{(j)} + \bar{j}_p^{(j)} \cos \vartheta^{(j)}. \end{aligned} \quad (17)$$

Since $d\bar{l}^{(j)}/d\vartheta^{(j)} = \bar{g}^{(j)}(\vartheta^{(j)})$ then the direction of the vector $\bar{g}^{(j)}(\vartheta^{(j)})$ is determined by the counterclockwise rotation viewed from the positive direction of the axis $O_p^{(j)} z_p^{(j)}$ and it is tangent to the directed circle (determined by the directed cylinder $C^{(j)}$). By using $\bar{r}_p^{(j)} = x_p^{(j)} \bar{i}_p^{(j)} + y_p^{(j)} \bar{j}_p^{(j)}$, for the cross-section of the conic convolute surface $\Sigma_I^{(j)}$ (following equations (16)) it can be written:

$$\bar{r}_p^{(j)} = r_0^{(j)} \bar{l}^{(j)}(\vartheta^{(j)}) - b^{(j)} \vartheta^{(j)} \bar{g}^{(j)}(\vartheta^{(j)}). \quad (18)$$

Let the cross-section of $\Sigma_I^{(j)}$ in the coordinate plane $O_p^{(j)} x_p^{(j)} y_p^{(j)}$ is illustrated, i.e. for the case $C_{z_p}^{(j)} = 0$, when

$$b^{(j)} = -\frac{p^{(j)}}{\cot \xi^{(j)}} > 0.$$

The above condition and the vector equality (18), determine the type of the cross-section of the studied conic convolute helicoids $\Sigma_I^{(j)}$, shown correspondingly in Fig. 6 [11].

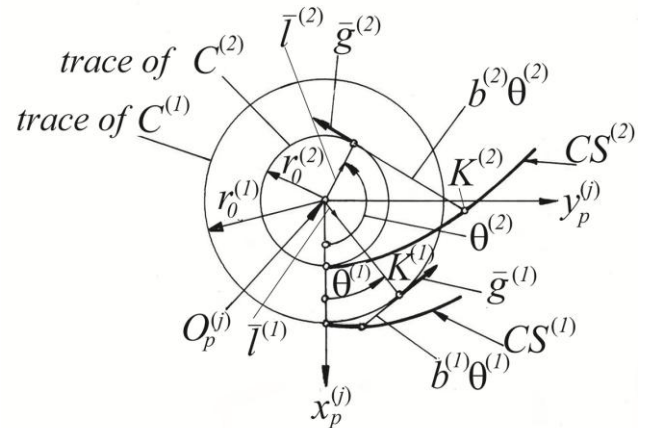


Fig. 6 Cross-section of the conic convolute helicoids $\Sigma_I^{(j)}$ of I type: $CS^{(j)}$ - line of the cross-section of the $\Sigma_I^{(j)}$

Axial section and axial angle of $\Sigma_I^{(j)}$. The equation of the axial section is obtained after the substitution of $y_p^{(j)} = 0$ in (2):

$$x_p^{(j)} = \frac{r_0^{(j)}}{\cos \vartheta^{(j)}} = r_0^{(j)} \sec \vartheta^{(j)}, \quad (19)$$

$$z_p^{(j)} = -p^{(j)} \text{conv}(\vartheta^{(j)}, k^{(j)}),$$

where $k^{(j)} = -\frac{r_0^{(j)}}{p^{(j)}} \cdot \cot \xi^{(j)} > 0,$

$$\text{conv}(\vartheta^{(j)}, k^{(j)}) = k^{(j)} \tan \vartheta^{(j)} - \vartheta^{(j)}.$$

The analytical type (19) of the axial section of the helicoid described by system (2) corresponds to its special geometry of a conic convolute helical surface, which is generated according to Fig. 1.

$$\frac{dx_p^{(j)}}{d\vartheta^{(j)}} = r_0^{(j)} \frac{\sin \vartheta^{(j)}}{\cos^2 \vartheta^{(j)}}, \quad \frac{dz_p^{(j)}}{d\vartheta^{(j)}} = -p^{(j)} \frac{k^{(j)} - \cos^2 \vartheta^{(j)}}{\cos^2 \vartheta^{(j)}}$$

$$\frac{dz_p^{(j)}}{dx_p^{(j)}} = -\frac{p^{(j)} k^{(j)} - \cos^2 \vartheta^{(j)}}{r_0^{(j)} \sin \vartheta^{(j)}}, \quad (20)$$

$$\frac{d^2 z_p^{(j)}}{dx_p^{(j)2} } = -\frac{p^{(j)} \cos^3 \vartheta^{(j)} (1 - k^{(j)} + \sin^2 \vartheta^{(j)})}{(r_0^{(j)})^2 \sin^3 \vartheta^{(j)}}.$$

Since the axial section of $\Sigma_1^{(j)}$, in the most common case, is asymmetric, the study is carried out for $\vartheta^{(1)} \in [0, \pi/2)$ and $\vartheta^{(2)} \in (-\pi/2, 0]$.

When $\vartheta^{(j)} = 0$, $x_p^{(j)} = r_0^{(j)}$ and $z_p^{(j)} = 0$, this point corresponds to the peak of the "axial section" curve. When $\vartheta^{(j)}$ varies from 0 to $\pm \pi/2$, $x_p^{(j)}$ grows from $r_0^{(j)}$ to $+\infty$, and $z_p^{(j)}$ changes to $\pm \infty$. Therefore, the graphics of the curves of the axial section (19) have asymptotes of the form:

$$z_p^{(j)} = A^{(j)} x_p^{(j)} + B^{(j)},$$

$$A^{(j)} = \lim_{x_p^{(j)} \rightarrow \infty} \frac{z_p^{(j)}(x_p^{(j)})}{x_p^{(j)}} = \pm \cot \xi^{(j)}, \quad (21)$$

$$B^{(j)} = \lim_{x_p^{(j)} \rightarrow \infty} [z_p^{(j)} - A^{(j)} x_p^{(j)}] = \pm p^{(j)} \frac{\pi}{2}.$$

Then the equations of the asymptotes of the curves, constituting the axial section of $\Sigma_1^{(j)}$ are of the form

$$z_p^{(j)} = \pm \cot \xi^{(j)} x_p^{(j)} \pm p^{(j)} \frac{\pi}{2}, \quad (j=1, 2), \quad (22)$$

and for $j=1$ the upper signs are valid, and for $j=2$ - the lowers ones.

When the angle $\delta^{(j)} = \xi^{(j)} - \pi/2$ is introduced (see Fig. 7 and Fig. 8), then the equation (22) takes the form:

$$z_p^{(j)} = \mp \tan \delta^{(j)} x_p^{(j)} \pm p^{(j)} \cdot \pi/2. \quad (23)$$

The points of intersection of the asymptotes with the coordinate axis $O_p^{(j)} z_p^{(j)}$ are determined from (23). Their applicate (z-axes) are:

$$z_p^{(j)} = \pm p^{(j)} \cdot \pi/2, \quad (24)$$

The points of intersection of the asymptotes with the axis $O_p^{(j)} x_p^{(j)}$ have abscissas defined by equality:

$$x_p^{(j)} = \frac{p^{(j)}}{\tan \delta^{(j)}} \cdot \frac{\pi}{2} = \frac{r_0^{(j)} \pi}{2k^{(j)}}. \quad (25)$$

The inflection points of the curves of the axial section are obtained from the condition

$$\frac{d^2 z_p^{(j)}}{dx_p^{(j)2} } = 0. \quad (26)$$

Considering (20), the condition (26) is satisfied, if $\cos^3 \vartheta^{(j)} (1 - k^{(j)} + \sin^2 \vartheta^{(j)}) = 0$, i.e. when

$$\vartheta^{(j)} = \pm \arcsin \sqrt{k^{(j)} - 1} \quad \left(\vartheta^{(j)} \neq \pm \frac{\pi}{2} \right). \quad (27)$$

If the condition $\vartheta^{(j)} = \pm \pi/2$ is fulfilled, the inflection points of the curves of the axial section go into $\pm \infty$. If condition (27) is satisfied, these points will exist for

$$1 < k^{(j)} < 2. \quad (28)$$

The form of the curves of the axial section of the conic convolute helicoid $\Sigma_1^{(j)}$ is analyzed both for the case defined by condition (28).

Case $k^{(j)} = \pi/2$. According to (27) and (28), in this case, there will be inflection points on the curves of the axial section that corresponds to $\vartheta^{(j)} = \pm \arcsin \sqrt{\pi/2 - 1}$ ($j=1, 2$). It follows from equality (25) that through the vertices of the curves delineating the axial section of $\Sigma_1^{(j)}$, their asymptotes go through. This case of an axial section is illustrated in Fig. 7 [11].

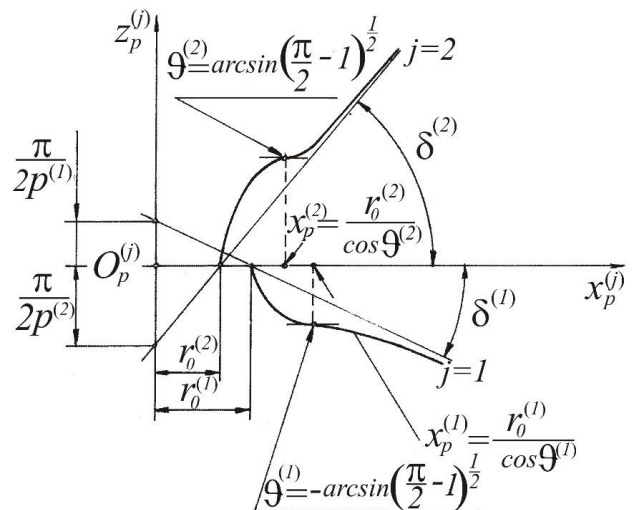


Fig 7 Curves of the axial section of conic convolute helicoids $\Sigma_1^{(j)}$ ($j=1, 2$) when $k^{(j)} = \pi/2$

Case $1 < k^{(j)} < \pi/2$. Applying the above reasoning, it can easily be seen that the curves of the axial section have the form illustrated in Fig. 8.

Each of the theoretical curves of the axial section of the conical convolute helicoid $\Sigma_1^{(j)}$, considered for the entire interval of $\vartheta^{(j)}$ (i.e. when $\vartheta^{(j)} \in [0, \pi/2)$ and $\vartheta^{(j)} \in (-\pi/2, 0]$, ($j=1, 2$)) is symmetrical to the axis $O_p^{(j)} x_p^{(j)}$ and has a nodal point, at $\vartheta^{(j)} = \vartheta_1^{(j)}$, which has the following coordinates:

$$x_p^{(j)} = \frac{r_0^{(j)}}{k^{(j)}} \cdot \frac{\vartheta_1^{(j)}}{\sin \vartheta_1^{(j)}}, \quad (30)$$

$$z_p^{(j)} = 0.$$

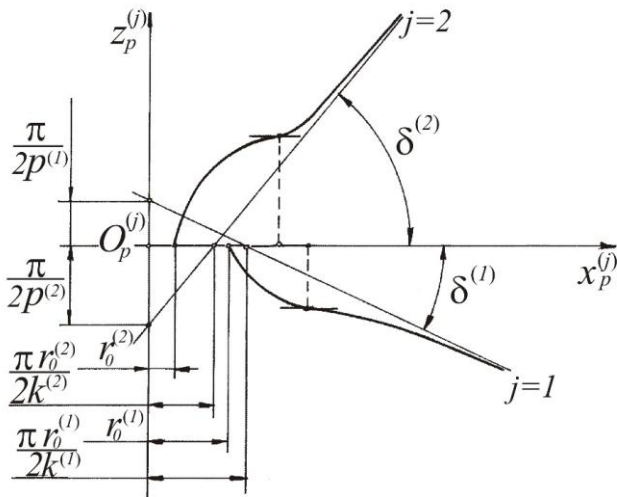


Fig 8. Curves of the axial section of conic convolute helicoids $\Sigma_1^{(j)}$ when $l < k^{(j)} < \pi/2$

In the considered case, the asymptotes of the axial section $\Sigma_1^{(j)}$, defined by equations (22) and (23), cross the axis $O_p^{(j)}x_p^{(j)}$ at points defined by the expression (25).

From the comparison of (25) and (30), it follows that the abscissas of the points of intersection of the curves of the axial section of the conic convolute helicoid $\Sigma_1^{(j)}$ ($j = 1, 2$) with the axes $O_p^{(j)}x_p^{(j)}$ are smaller than those of the points of intersection with the asymptotes with the same axis, due to the fact known from mathematics that

$$l > \frac{\sin \vartheta^{(j)}}{\vartheta^{(j)}} \geq \frac{2}{\pi}, \quad \text{for } \vartheta^{(j)} \in [-\pi/2, 0) \quad \text{and} \quad \vartheta^{(j)} \in (0, \pi/2].$$

The axial angle $\alpha_s^{(j)}$ in an arbitrary point of the axial section of the studied conic helicoid is obtained from the equations system (20):

$$\tan \alpha_s^{(j)} = \left| \frac{dz_p^{(j)}}{dx_p^{(j)}} \right| = \left| -\frac{p^{(j)}}{r_0^{(j)}} \cdot \frac{k^{(j)} - \cos^2 \vartheta^{(j)}}{\sqrt{1 - \cos^2 \vartheta^{(j)}}} \right|, \quad (31)$$

where $k^{(j)} = -\frac{r_0^{(j)}}{p^{(j)}} \cot \xi^{(j)}$, $\cos \vartheta^{(j)} = \frac{r_0^{(j)}}{x_p^{(j)}}$,

Then

$$\alpha_s^{(j)} = \arctan \left| \frac{p^{(j)} \frac{r_0^{(j)}}{x_p^{(j)}} + x_p^{(j)} \cot \xi^{(j)}}{\sqrt{x_p^{(j)2} - r_0^{(j)2}}} \right|, \quad (32)$$

After substitution of $x_p^{(j)} = r_p^{(j)}$ into (32), it is obtained the axial angle of $\Sigma_1^{(j)}$ in a point in an arbitrary conic surface, coaxial with the outer surface of the conic gear equipped with convolute helical teeth of the studied type.

4. Singular Contact Points on Conic Linear Helicoids

It is known [13, 14] that for the cases prevailing in technological practice when generating cylindrical worms and cylindrical worm cutters, whose tooth surfaces are linear helicoids, knives are used as cutting tools, the cutting edges of which are arranged in a certain way relative to the geometric axis (axis of rotation) of the generated product.

The cutting edges of the knives represent the generatrix lines $\Sigma^{(j)}$ ($j = 1, 2$) (Fig. 1) that generate the linear surfaces. This technological approach is also applicable in the practical implementation of conical linear helicoids [2].

Conic convolute helicoid. To prevent the phenomenon of "undercutting" of the active tooth surfaces of gear transmissions and instruments, representing parts of conic linear helicoids, during their generation, it is necessary to define conditions for the appearance of the ordinary points (points of undercutting) on them. As already illustrated, the conic linear helicoids $\Sigma_1^{(j)}$ ($j = 1, 2$) (and in particular the conic convolute helical surface) have the form: $\bar{\rho}_1^{(j)} = \bar{\rho}_1^{(j)}(u^{(j)}, \vartheta^{(j)})$.

Then the normal vector $\bar{n}_1^{(j)}$ at $\Sigma_1^{(j)}$ ($j = 1, 2$) in an arbitrary point $N^{(j)}$ is defined by

$$\bar{n}_1^{(j)} = \frac{\partial \bar{\rho}_1^{(j)}}{\partial u^{(j)}} \times \frac{\partial \bar{\rho}_1^{(j)}}{\partial \vartheta^{(j)}}, \quad (33)$$

where $\frac{\partial \bar{\rho}_1^{(j)}}{\partial u^{(j)}}$ and $\frac{\partial \bar{\rho}_1^{(j)}}{\partial \vartheta^{(j)}}$ are vectors in point $N_1^{(j)}$ from the conic helical surface $\Sigma_1^{(j)}$, tangent to the coordinate lines $u^{(j)} = \text{constant}$ and $\vartheta^{(j)} = \text{constant}$.

It is known [12], that point $N^{(j)}$ from $\Sigma_1^{(j)}$ is singular (node), if in it a normal vector $\bar{n}_1^{(j)}$ cannot be defined, i.e. the following condition is fulfilled:

$$\bar{n}_1^{(j)} = \bar{0}. \quad (34)$$

Then from (2), for the projections of the normal vector $\bar{n}_1^{(j)}$ in the coordinate system $S_p^{(j)}$ can be written:

$$\begin{aligned} n_{1,x_p}^{(j)} &= \mp h^{(j)} \sin \xi^{(j)} \cos \vartheta^{(j)} - D \cos \xi^{(j)} \sin \vartheta^{(j)}, \\ n_{1,y_p}^{(j)} &= \mp h^{(j)} \sin \xi^{(j)} \sin \vartheta^{(j)} + D \cos \xi^{(j)} \cos \vartheta^{(j)}, \\ n_{1,z_p}^{(j)} &= D \sin \xi^{(j)}. \end{aligned} \quad (35)$$

$$D = (u^{(j)} \sin \xi^{(j)} - p_t^{(j)} \vartheta^{(j)})$$

From (35) it can be seen, that condition (34) is never satisfied for the conic convolute helicoid, since $h^{(j)} \neq 0$. This means that the conic convolute helicoid consists of only non-singular points.

5. Conclusion

Basic analytical and geometrical synthesis of conic convolute helicoids is realized. The obtained equations show a theoretical possibility, depending on the basic geometrical characteristics of the

designed conic convolute worm, to generate the active surfaces of its helical teeth as parts of the intended pairs of conic convolute helicoids. In this study are shown the analytical dependences of the cross-section and the axial section, which are important for the synthesis of the conic helical surfaces. On the base of the realized studies, is created a computer program, for illustrations of these helicoids. The illustrated, in this work, equations of conic helicoids, as well as the analytical descriptions of their cross-sections and axial sections, are important geometric characteristics of the active tooth surfaces of conic worms or conic hobs. They are related to the technological synthesis of gear mechanisms with the application of these new types of helical surfaces operating in the condition of working and/or instrumental meshing. The notes made about the appearance of undercutting cutting points on these surfaces, with the chosen generation approach, are also particularly essential for their technological synthesis.

6. Acknowledgment

This work has been accomplished with the financial support by the Grant No BG05M2OP001-1.002-0011-C02 financed by the Science and Education for Smart Growth Operational Program (2014-2020) and co-financed by the European Union through the European structural and Investment funds.

7. References

1. E. Abadjieva. Spatial Rack Drives. Mathematical Modelling for Synthesis. VDM Verlag Dr. Müller e.K., 2011, 72 pp., (ISBN: 978-3-639-24045-0)
2. V. Abadjiev. Gearing Theory and Technical Applications of Hyperboloid Drives, Sc. D. Thesis, Institute of Mechanics, Bulgarian Academy of Sciences, Sofia, 309, (2007),(in Bulgarian)
3. Abadjieva, E., V. Abadjiev. Regular Mechanical Transformation of Rotations into Translations: Part 2. Kinematic Synthesis of the Elements of High Kinematic Joints, Realizing the Process of Motions Transformations. J. of Theor. and Appl. Mech., Sofia, 47(3), 3-24 (2017)
4. Lashnev, S., Yulikov, M. Calculation and Design of Metal-Cutting Tools with an IBM Application. Mashinostroenie, Moscow, 391, (1975)
5. Litvin, F., Fuentes, A. Gear Geometry and Applied Theory. Second Edition, Cambridge University Press, 800, (2004)
6. Lyukshin, V. The Theory of Helical Surfaces in the Design of Cutting Tools. Mashinostroenie Publishing House, Moscow, 371, (1968)
7. Semchenko, I., Magyushin, M., G. Saharov. Design of Metal Cutting Tools. Mashgiz, Moscow, 952, (1962)
8. Abadjiev, V., Okhotsimsky, D., Platonov, A. Research on the Spatial Gears and Applications, Keldysh Institute of Applied Mathematics, Russian Academy of Sciences, Preprint No 89, Moscow, (1997).
9. BDS 8540-84, 1985. Gear sets. Common terms. Definitions and symbols. Institute of Standardization, Sofia, (1985).
10. Abadjiev, V. Mathematical Modelling for Synthesis of Spatial Gears, Journal of Process Mechanical Engineering., Proc Inst. Mech Engrs, Vol. 216, Part E, pp. 31-46, (2002).
11. Abadjiev V., E. Abadjieva. Conic Linear Helicoids: Part 1. Synthesis and Analysis of the Basic Geometric Characteristics. Gears in Design, Production, and Education. Mechanisms and Machine Science, 101. Springer, Cham, 339-360, (2021)
12. Rashevsky, P. Course of Differential Geometry. Ed. State Publishing House of Technical and Theoretical Literature, Moscow, 1956, 420, (1956).
13. Ginzburg, E., N. Golovanov, N. Firun, N. Halebsky. Gear Transmissions. Mashinostroenie, Leningrad, 416, (1980)
14. Golovanov, N., E. Gizburg, N. Firun Spatial Transmissions, and Worm Gear Mechanisms. Mashinostroenie, Leningrad, 515, (1967).